Precise determination of excitation energies in condensed-phase molecular systems based on exciton-polariton measurements

Nguyen Thanh Phuc* and Akihito Ishizaki

Department of Theoretical and Computational Molecular Science, Institute for Molecular Science, Okazaki 444-8585, Japan and Department of Structural Molecular Science, Graduate University for Advanced Studies, Okazaki 444-8585, Japan

(Received 23 April 2019; revised manuscript received 21 August 2019; published 11 October 2019)

The precise determination of the excitation energies in condensed-phase molecular systems is important for understanding system-environment interactions as well as for the prerequisite input data of theoretical models used to study the dynamics of the system. The excitation energies are usually determined by fitting of the measured optical spectra that contain broad and unresolved peaks as a result of the thermally random dynamics of the environment. Herein, we propose a method for precise energy determination by strongly coupling the molecular system to an optical cavity and measuring the energy of the resulting polariton. The effect of thermal fluctuations induced by the environment on the polariton is also investigated, from which a power scaling law relating the polariton's linewidth to the number of molecules is obtained. The power exponent gives important information about the environmental dynamics.

DOI: 10.1103/PhysRevResearch.1.033019

I. INTRODUCTION

Embedded in the high density of environmental particles, the excitation energies of molecules in the condensed phase can be modified from their values in the gas phase by the static influence of various kinds of system-environment interactions [1,2] including electrostatic interaction and hydrogen bonding [3–8], as well as the effects of molecular conformation [9,10]. Therefore, a precise determination of the excitation energies of condensed-phase molecular systems is significant for the understanding of system-environment interactions. Moreover, these energy values are also prerequisite as input parameters for almost all theoretical models used to study the dynamics of molecular systems [11,12]. The excitation energies of condensed-phase molecular systems are usually determined by fitting of the measured optical spectra. The optical spectra, however, often contain broad and unresolved peaks as a result of the thermally random dynamics of the environment interacting with the molecular system. Moreover, to extract excitation energy information from the optical spectra, it is necessary to develop a theory of optical spectra that addresses the often sophisticated spectral density of the environment. A variety of approximations are sometimes used to reduce the complexity of the calculations [11,13,14]. Consequently, it is desirable to develop an alternative approach that can precisely determine the excitation energies of condensed-phase molecular systems without requiring detailed information about the environmental random dynamics.

In this paper we propose a method for the precise determination of the excitation energies of condensed-phase molecular systems by strongly coupling the molecules to an optical cavity and measuring the energy of the polariton that results from the hybridization of the degrees of freedom of light and matter. Strong coupling of molecules to an optical cavity has already been realized in many experimental platforms [15–25]. It has led to a variety of interesting phenomena and important applications including the control of chemical reactivity [26–33], enhancement of transport [34–39], nonlinear optical properties of organic semiconductors with applications to optoelectronic devices [40–43], and polariton lasing and condensate [44–47].

The underlying mechanism that allows a precise determination of the excitation energies of condensed-phase molecular systems is that the polariton appears as a sharp peak in optical spectra under the strong coupling between the cavity mode and the electronic excitations of molecules. This is related to the effect of vibronic or polaron decoupling found in the Holstein-Tavis-Cummings (HTC) model that describes molecules with a single vibrational mode that are coupled to an optical cavity [28,48–51] and the extended model [52]. However, since the polariton is a superposition state involving a large number of electronic excitations of molecules [see Eq. (4)] and therefore can be vulnerable to decoherence, the effect of thermal fluctuations induced by the environment on the polariton state at finite temperatures, which is not captured in the HTC model and its extension, is a nontrivial and important issue.

In this paper, by investigating the effect of thermal fluctuations induced by the environment on the polariton, a power scaling law relating the polariton's linewidth to the number of molecules coupled to the cavity is determined. The power exponent strongly depends on the environment's dynamic timescale. As such, information on environmental dynamics can be extracted from the polariton spectrum obtained for a

*Corresponding author: nthanhphuc@ims.ac.jp

variable number of molecules. Since the polariton contains both light and matter degrees of freedom, its energy can be obtained by either cavity-transmission or molecular-absorption spectroscopies. In the latter, the polariton needs to be in a bright state with respect to molecular absorption. However, this condition is not satisfied if there are pairs of molecules with the opposite orientations, such as in the case of random orientations. The effective Rabi frequencies for an ensemble of identical molecules or molecular complexes with random orientations are derived. The molecular-absorption and cavity-transmission spectroscopies are calculated for molecular systems with different types of orientations.

II. EFFECT OF THERMAL FLUCTUATIONS ON THE LOWER POLARITON'S OPTICAL SPECTRUM

We first consider a system of N identical molecules whose electronic excitations are coupled to a single mode of an optical cavity (Fig. 1) via dipole interaction

$$\hat{H}_{\mathrm{m-c}} = \frac{\hbar\Omega_{\mathrm{R}}}{2}\sum_{m=1}^{N}(|\mathrm{e}_m\rangle\langle \mathrm{g}_m|\hat{a} + |\mathrm{g}_m\rangle\langle \mathrm{e}_m|\hat{a}^{\dagger}), \tag{1}$$

where Ω_{R} is the single-emitter Rabi frequency that characterizes the coupling strength between the cavity and a molecule, $\hat{a}$ denotes the annihilation operator of the cavity photon, and $|\mathrm{g}_m\rangle$ and $|\mathrm{e}_m\rangle$ represent the electronic ground and excited states, respectively, of the mth molecule. We first assume that all molecules inside the cavity have the same orientation such that their Rabi couplings are equal. The case of molecules with different orientations will be considered later.

Each molecule in condensed phase is assumed to be coupled to an independent environment, which is modeled by an ensemble of harmonic oscillators $\hat{H}_{\mathrm{e}} = \sum_{m=1}^{N}\sum_{\xi}\hbar\omega_{m,\xi}\hat{b}^{\dagger}_{m,\xi}\hat{b}_{m,\xi}$, where $\omega_{m,\xi}$ and $\hat{b}_{m,\xi}$ represent the frequency and annihilation operator of the ξ mode of the environment surrounding the mth molecule. The dynamics of the environment at a finite temperature induces energy fluctuations in the electronic excited states of the molecules

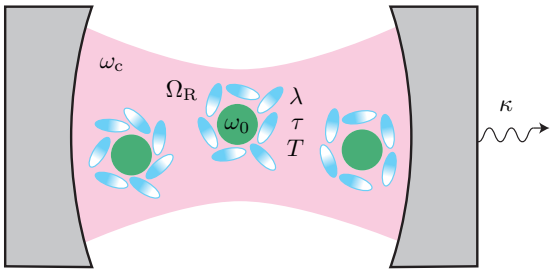

FIG. 1. Schematic illustration of a system of condensed-phase molecules coupled to a single mode of an optical cavity (light magenta) with frequency ω_{c} and decay rate κ. Each molecule (green sphere) with the electronic excitation energy $\hbar\omega_0$ interacts with an independent surrounding environment represented by blue ellipsoids. The thermal dynamics of the environments at a finite temperature T induces energy fluctuations in the molecules that are characterized by the reorganization energy λ and the relaxation timescale τ. The coupling strength between the cavity and a molecule is given by the single-emitter Rabi frequency Ω_{R}.

as given by the Hamiltonian [1]

$$\hat{H}_{\mathrm{m-e}} = \sum_{m=1}^{N}\left[\hbar\omega_0 + \sum_{\xi} g_{m,\xi}(\hat{b}^{\dagger}_{m,\xi} + \hat{b}_{m,\xi})\right]|\mathrm{e}_m\rangle\langle \mathrm{e}_m|. \tag{2}$$

Here, $\hbar\omega_0$ is the molecule's excitation energy and $g_{m,\xi}$ denotes the coupling strength between the mth molecule and the ξ mode of the environment. The dynamics of the environment is characterized by the relaxation function $\Psi_m(t) = (2/\pi)\int_0^{\infty} d\omega J_m(\omega)\cos(\omega t)/\omega$, where $J_m(\omega) = \pi\sum_{\xi} g^2_{m,\xi}\delta(\omega - \omega_{m,\xi})$ is the spectral density. When the spectral density is given by the Drude-Lorentz form, $J_m(\omega) = 2\lambda_m\tau_m\omega/(\tau_m^2\omega^2 + 1)$, the relaxation function has an exponential form, $\Psi_m(t) = 2\lambda_m\exp(-t/\tau_m)$, where λ_m is the environmental reorganization energy, which is usually employed to characterize the system-environment coupling strength, and τ_m is the characteristic timescale of the environmental relaxation or reorganization process [53]. The time evolution of the system's reduced density operator can be solved in a numerically accurate fashion using the hierarchical equations of motion approach, for example [54].

The molecular absorption spectrum can be expressed in terms of the system's dynamical quantities as [55]

$$\mathcal{A}(\omega) = \mathrm{Im}\left\{\frac{i}{\hbar}\int_0^{\infty} dt\, e^{i\omega t}\mathrm{Tr}[\hat{\mu}\mathcal{G}(t)\hat{\mu}^{\times}\hat{\rho}_0]\right\}, \tag{3}$$

where $\hat{\mu} = \sum_{m=1}^{N}(\mu_m|\mathrm{e}_m\rangle\langle \mathrm{g}_m| + \mu_m^*|\mathrm{g}_m\rangle\langle \mathrm{e}_m|)$ is the total transition dipole moment operator with μ_m being the matrix element of the transition dipole moment of the mth molecule, and $\hat{\mu}^{\times}\hat{\rho} \equiv \hat{\mu}\hat{\rho} - \hat{\rho}\hat{\mu}$. Here, the density operator $\hat{\rho}_0 = |\mathrm{G}\rangle\langle \mathrm{G}|$ with $|\mathrm{G}\rangle = \prod_{m=1}^{N}|\mathrm{g}_m\rangle \otimes |0\rangle_{\mathrm{c}}$ being the ground state of the cavity-molecule system. The superoperator $\mathcal{G}(t)$ describes the time evolution of the system in Liouville space, which is numerically obtained by solving the hierarchical equation of motion [54]. It should be noted that Eq. (3) takes into account both the intermolecular interaction and the molecule-environment interaction. In the following numerical demonstration, we set $\omega_0 = 12400\ \mathrm{cm}^{-1}$, $\lambda = 50\ \mathrm{cm}^{-1}$, $\tau = 100$ fs, and $T = 300$ K, which are typical values in photosynthetic pigment-protein complexes [11,12]. The cavity frequency is taken to be $\omega_{\mathrm{c}} = 12450\ \mathrm{cm}^{-1}$, i.e., with a detuning of $50\ \mathrm{cm}^{-1}$ from the molecule's excitation energy. The cavity's Q factor ($\kappa = \omega_{\mathrm{c}}/Q$) is set to be $Q = 10^4$, a typical value for microcavities used in cavity QED experiments [56]. When many molecules are coupled to a single mode of the optical cavity, it is the collective Rabi coupling $\sqrt{N}\Omega_{\mathrm{R}}$ that determines the polariton energy.

To investigate the effect of thermal fluctuation induced by the environment on the polariton, we numerically calculate the full width at half maximum (FWHM) of the lower polariton (LP) peak in the molecular-absorption spectrum using Eq. (3). It is determined that in the absence of molecule-cavity coupling, the molecular absorption peak has a broad linewidth of approximately $291\ \mathrm{cm}^{-1}$ due to strong thermal fluctuation, which is larger than the typical separation between absorption peaks of a photosynthetic complex [11]. However, as shown in Fig. 2, when the molecules are coupled to the cavity mode with $\sqrt{N}\Omega_{\mathrm{R}} = 0.1$ eV, which is sufficiently large compared with λ and $k_{\mathrm{B}}T$, the LP linewidth $\Delta\nu_{\mathrm{LP}}$ reduces significantly

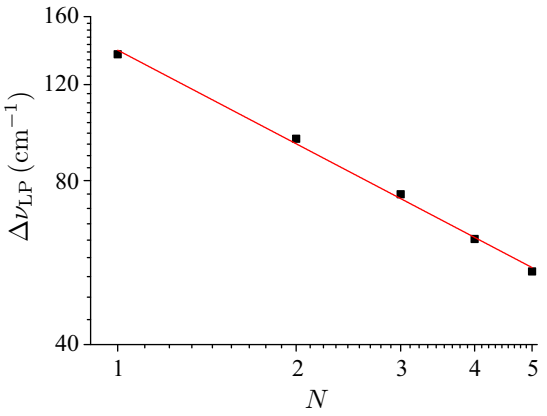

FIG. 2. Dependence of the linewidth $\Delta\nu_{\rm LP}$ of the LP peak in the molecular absorption spectrum on the number N of molecules coupled to the cavity mode. Here both axes are shown in the logarithmic scales. The red line is the linear fitting of the numerical data. The optical cavity has $Q = 10^4$.

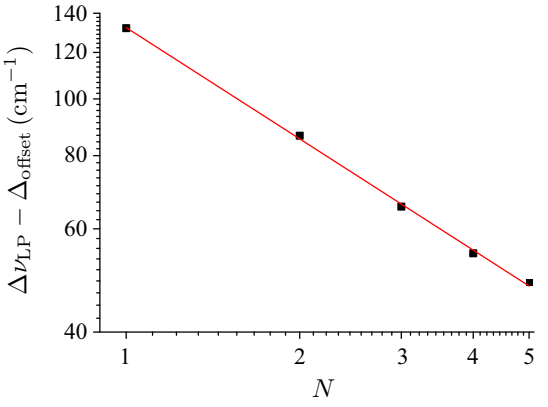

FIG. 3. $\Delta\nu_{\rm LP} - \Delta_{\rm offset}$ vs N for a cavity with $Q = 33.34$. Here $\Delta_{\rm offset} = 150\,{\rm cm}^{-1}$.

with an increase of the number N of molecules. A power scaling law $\Delta\nu_{\rm LP} = \Delta_0 N^{-\alpha}$ is determined with $\Delta_0 = 138 \pm 4\,{\rm cm}^{-1}$ and $\alpha = 0.57 \pm 0.02$ obtained via the linear fitting of numerical data in the logarithmic scale.

To obtain physical insight into the effect of thermal fluctuations on the LP, we perform an analysis by first assuming that the effect of the environment does not alter the structure of the LP, which, in the strong-coupling regime $\sqrt{N}\Omega_{\rm R} \gg \lambda$, has an approximate form of [51]

$$|{\rm LP}\rangle = c_1 \prod_{m=1}^{N} |{\rm g}_m\rangle \otimes |1\rangle_{\rm c} + c_2 |{\rm B}\rangle \otimes |0\rangle_{\rm c}, \tag{4}$$

where c_1 and c_2 satisfy $|c_1|^2 + |c_2|^2 = 1$. Here, $|n\rangle_{\rm c}$ denotes the Fock state with n cavity photons and $|{\rm B}\rangle = (1/\sqrt{N})\sum_{m=1}^{N} |{\rm e}_m\rangle$ is the bright state, which is a superposition of electronic excitations of all molecules coupled to the cavity. This is a superposition state involving electronic excitations from all molecules inside the cavity. Given that each of the molecular electronic excitations $|{\rm e}_m\rangle$ is coupled to the environmental modes via the interaction given by Eq. (2), the LP with the aforementioned structure can be regarded as having an effective interaction with the environment in which the number of modes is multiplied by a factor of N while the coupling strength to each mode is reduced by a factor of $(1/\sqrt{N})^2 = 1/N$. As a result, the effective reorganization energy $\lambda_{\rm LP}$ for the LP is multiplied by a factor of $1/N$ because the spectral density is proportional to the mode density and the coupling strength squared.

The effect of the environment on the LP's linewidth depends on the timescale of environmental dynamics. In the inhomogeneous broadening limit $\sqrt{k_{\rm B}T\lambda_{\rm LP}} \gg \tau^{-1}$, which corresponds to a slow environmental dynamics, the line shape has a Gaussian form and the linewidth is characterized by the amplitude of fluctuations in the environment $\Delta\nu_{\rm LP} \propto \sqrt{k_{\rm B}T\lambda_{\rm LP}}$ as τ becomes irrelevant. As a result, the LP linewidth follows an $N^{-1/2}$ scaling. In the opposite limit of homogeneous broadening $\sqrt{k_{\rm B}T\lambda_{\rm LP}} \ll \tau^{-1}$, which corresponds to a fast environmental dynamics, the LP peak gets sharper due to the motional line narrowing phenomenon [57] and the line shape has a Lorentzian form with the linewidth given by $\Delta\nu_{\rm LP} \propto k_{\rm B}T\lambda_{\rm LP}\tau$ [1]. As a result, the LP's linewidth follows an N^{-1} scaling.

To examine the validity of the preceding analysis, in which it was assumed that thermal fluctuations do not affect the structure of the LP, we numerically calculate the N dependence of the LP linewidth for different values of the reorganization energy λ using Eq. (3). It was determined that the power scaling law $\Delta\nu_{\rm LP} \propto N^{-\alpha}$ is well satisfied with a strong λ dependence of the power exponent as shown in Fig. 4. Consequently, environmental dynamics information can be extracted from the power exponent α obtained by measuring the LP spectrum for a variable number of molecules coupled to the cavity. It is evident from Fig. 4 that α generally decreases with an increase of λ and tends to approach a steady value close to the analytical result of $\alpha = 1$ ($\alpha = 0.5$) in the inhomogeneous (homogeneous) broadening limit. This implies that the superposition state of the LP given by Eq. (4) is not largely destroyed by thermal fluctuations provided that the collective Rabi coupling $\sqrt{N}\Omega_{\rm R}$ is large compared with both the reorganization energy λ and the temperature $k_{\rm B}T$. However, the residual discrepancy between numerical and analytical results of α should be attributed to the effect of thermal fluctuations on the structure of the LP.

Since the LP is formed by a coupling between the molecules and the optical cavity, its linewidth should depend on the cavity's photonic leakage. The larger the Q factor, the sharper the LP peak, and thus the more precise the measurement. It turns out, however, that even for cavities with small Q factors ($Q \sim 10$), which are often used in molecular polariton experiments [15], the power scaling law remains valid by introducing an offset, $\Delta\nu_{\rm LP} = \Delta_{\rm offset} + \Delta_0 N^{-\alpha}$. This is obvious from the linear relation between $\Delta\nu_{\rm LP} - \Delta_{\rm offset}$ and N shown in Fig. 3 for $Q = 33.34$, where both axes are in logarithmic scales. Using the linear fitting procedure, we obtain $\Delta_{\rm offset} \simeq 150\,{\rm cm}^{-1}$. It is evident that $\Delta_{\rm offset}$ is smaller than the cavity loss $\kappa = \omega_c/Q$, which is in agreement with the experimental observation that the lifetime of the coupled state can be longer than that of uncoupled constituents [58–62].

It should be noted that the setup for a precise determination of molecular excitation energies proposed in this paper differs

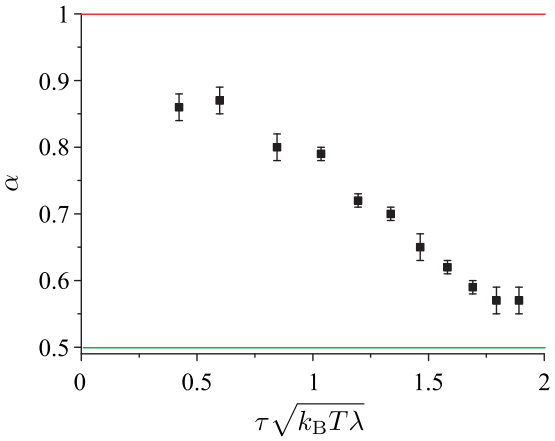

FIG. 4. Dependence of the power exponent α in the power scaling $\Delta\nu_{LP} \propto N^{-\alpha}$, relating LP linewidth to the number of molecules coupled to the cavity, on the dimensionless quantity $\tau\sqrt{k_B T\lambda}$ characterizing the environment's dynamic motion. Here, λ is the reorganization energy, τ is the relaxation timescale, and T is the temperature of the environment (k_B is the Boltzmann constant). The red (green) line indicates the value of $\alpha = 1$ ($\alpha = 0.5$), which is the value of α in the inhomogeneous (homogeneous) broadening limit $\tau\sqrt{k_B T\lambda} \ll 1$ ($\tau\sqrt{k_B T\lambda} \gg 1$) obtained from an analysis based on the assumption that thermal fluctuations do not affect the structure of the LP (see the main text for details).

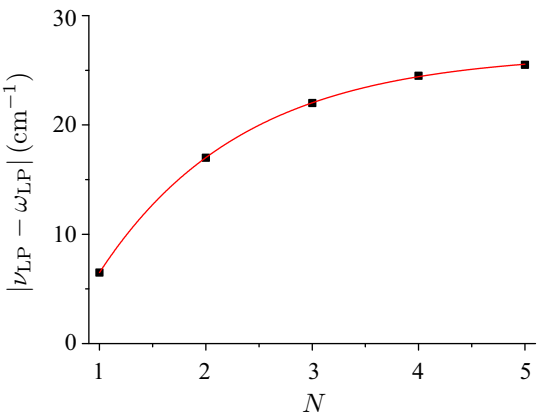

FIG. 5. Deviation $|\nu_{LP} - \omega_{LP}|$ of the position of the LP peak in the molecular absorption spectrum from its energy as a function of the number N of molecules coupled to the cavity. The red curve shows the exponential fitting of the numerical data to the function $|\nu_{LP} - \omega_{LP}| = A - Be^{-\gamma N}$.

from the typical setup in experiments studying molecular polariton relaxation dynamics, where a short laser pulse is used to excite the molecule to a broad band of states with high vibration numbers in the LP manifold [58–62]. Since the energies of high-vibration states are close to those of dark states (i.e., the bare molecular excitation energies), a transition from these states in the LP manifold to the dark states can occur. In contrast, in the setup for molecular-absorption spectrum (and also for cavity-transmission spectrum considered later), a continuous-wave (CW) laser with a monochromatic wavelength is used to excite the molecule to the lowest energy state in the LP manifold, which lies well below the dark states. Since the energy difference given by half of the collective Rabi frequency is large compared with the temperature in the strong-coupling regime under consideration, the probability for a transition from this excited state to the dark states should be negligibly small. In other words, even though the high-frequency vibrations can fill the energy difference, the number of high-frequency phonons in thermal equilibrium is so small that the transition to dark states via phonon absorption is inefficient. The interaction between multiple excitons can also be neglected in spectroscopic measurements using low-intensity light.

The LP energy can be obtained by diagonalizing the Hamiltonian of the cavity-molecule system, yielding

$$\omega_{LP} = \tfrac{1}{2}\big[\omega_c + \omega_0 - \sqrt{(\omega_c - \omega_0)^2 + N\Omega_R^2}\big]. \qquad (5)$$

For a sufficiently large collective Rabi frequency, $\sqrt{N}\Omega_R \gg |\omega_c - \omega_0|$, it reduces to $\omega_{LP} \simeq (\omega_c + \omega_0 - \sqrt{N}\Omega_R)/2$. Therefore, by repeating the measurement of the LP energy with variable molecular density, in which N is varied, or with variable number of photons in the cavity, by which Ω_R is varied, we can obtain the molecular excitation energy $\hbar\omega_0$ via a simple linear fitting, given that the cavity frequency ω_c is known, for example, based on the transmission spectroscopy measurement of the bare cavity.

As shown in Fig. 5, the deviation $|\nu_{LP} - \omega_{LP}|$ of the position of the LP peak in the absorption spectrum from its energy was determined to increase with an increase of the number N of molecules coupled to the cavity prior to saturation, following the function $|\nu_{LP} - \omega_{LP}| = A - Be^{-\gamma N}$. Using the exponential fitting procedure, we find the saturation value of $A \simeq 27\,\mathrm{cm}^{-1}$, which is smaller than $\Delta\nu_{LP} \simeq 55\,\mathrm{cm}^{-1}$ for $N = 5$ (see Fig. 2). This behavior of the deviation should also be attributed to the effect of thermal fluctuation on the structure of the LP. Indeed, under the ansatz Eq. (4) for the LP structure, the shift of the LP peak due to the environmental coupling should be between zero (in the homogeneous broadening limit) and λ_{LP} (in the inhomogeneous broadening limit) [1]. In the case that the collective Rabi frequency is large compared with the detuning, we have the coefficients $|c_1| \simeq |c_2| \simeq 1/\sqrt{2}$ in Eq. (4), for which $\lambda_{LP} \simeq \lambda/(4N)$. This value of λ_{LP} is much smaller than the deviation $|\nu_{LP} - \omega_{LP}|$ obtained numerically.

As for the Rabi-frequency dependence, the LP linewidth $\Delta\nu_{LP}$ decreases with an increase of Ω_R before it saturates at a sufficiently large collective Rabi frequency, as shown in Fig. 6 for $N = 3$. The saturation value is determined by the number of molecules coupled to the cavity. Meanwhile, the deviation $|\nu_{LP} - \omega_{LP}|$ follows a power scaling $|\nu_{LP} - \omega_{LP}| = C\Omega_R^{-\eta}$ as indicated by the linear relation in the logarithmic plot shown in Fig. 7 (for $N = 3$).

III. MOLECULAR COMPLEX

Next, we consider a molecular complex composed of molecules with different excitation energies and transition dipole moments. Both the magnitude and the sign of the Rabi coupling, which depend on the magnitude and direction of the molecule's transition dipole moment, can differ from one molecule to another in the system. In the following numerical

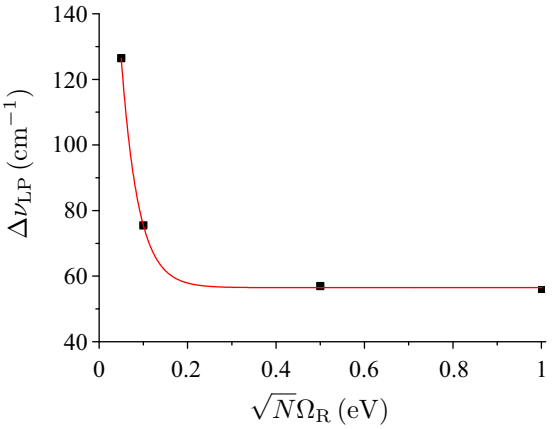

FIG. 6. Dependence of the LP linewidth $\Delta\nu_{\rm LP}$ on the collective Rabi frequency $\sqrt{N}\Omega_{\rm R}$. The red curve is the fitting of the numerical data following the function $\Delta\nu_{\rm LP} = A + Be^{-\gamma\Omega_{\rm R}}$.

demonstration, we consider a system of $N = 3$ molecules with excitation energies $\omega_1 = 12400\,{\rm cm}^{-1}$, $\omega_2 = 12500\,{\rm cm}^{-1}$, and $\omega_3 = 12600\,{\rm cm}^{-1}$. The Rabi frequencies associated with the three molecules are taken to be $\sqrt{N}\Omega_{\rm R}^{(1)} = 0.1$ eV, $\Omega_{\rm R}^{(2)} = \Omega_{\rm R}^{(1)}\sqrt{3}/2$, and $\Omega_{\rm R}^{(3)} = -\Omega_{\rm R}^{(1)}/\sqrt{2}$. We also consider coupling between electronic excitations of different molecules given by the Hamiltonian

$$\hat{H}_{\rm m-m} = \sum_{m\neq n} \hbar V_{mn} |{\rm e}_n\rangle\langle {\rm g}_n| \otimes |{\rm g}_m\rangle\langle {\rm e}_m|, \tag{6}$$

where the coupling matrix elements V_{mn} between the mth and the nth molecules satisfy $V_{mn} = V_{nm}^*$. Here, we take $V_{mn} = 50\,{\rm cm}^{-1}$.

As shown in Fig. 8, there is a relatively sharp and isolated peak in the molecular-absorption spectrum that corresponds to the LP. The linewidth of the peak is determined to be $\Delta\nu_{\rm LP} \simeq 85\,{\rm cm}^{-1}$. Besides the LP peak, there is a broad peak that contains the absorption spectra of the upper polariton as well as two other energy eigenstates. In the case of a system of identical molecules considered in the preceding section, these eigenstates are dark states with respect to molecular absorption, and thus they do not appear in the spectrum. Here, due to the difference in the excitation energy and Rabi coupling between molecules as well as the intermolecular electronic couplings, these eigenstates are no longer fully dark states. However, since these eigenstates mainly consist of molecular degrees of freedom, their spectra are broad and unresolved in comparison with the LP peak.

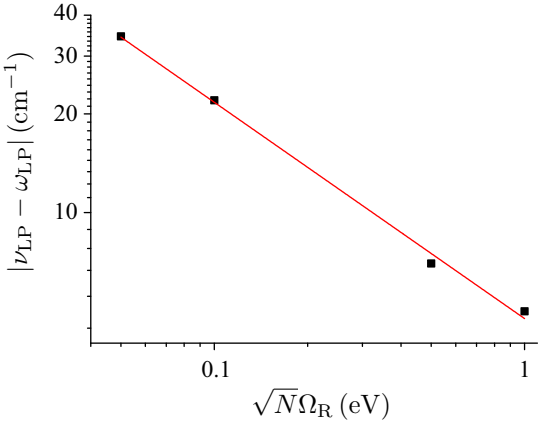

FIG. 7. Dependence of the deviation $|\nu_{\rm LP} - \omega_{\rm LP}|$ on the collective Rabi frequency $\sqrt{N}\Omega_{\rm R}$. Both axes are shown in the logarithmic scale. The red line is the linear fitting of the numerical data.

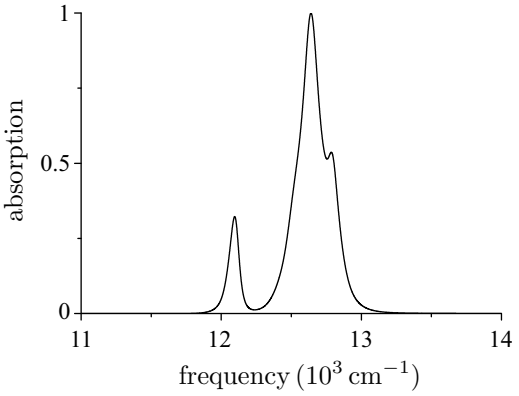

FIG. 8. Molecular-absorption spectrum of a system of $N = 3$ molecules with different excitation energies $\omega_1 = 12400$, $\omega_2 = 12500$, and $\omega_3 = 12600\,{\rm cm}^{-1}$ coupled to a single mode of an optical cavity with frequency $\omega_{\rm c} = 12450\,{\rm cm}^{-1}$. Here, the absorption is normalized by its maximum value. The electronic couplings between molecules are $V_{mn} = 50\,{\rm cm}^{-1}$ ($m, n = 1, 2, 3$). The environment and its coupling to the molecules are characterized by the reorganization energy $\lambda = 50\,{\rm cm}^{-1}$, the relaxation timescale $\tau = 100$ fs, and the temperature $T = 300$ K. The relatively sharp and isolated peak on the left corresponds to the LP, which can be used for a precise determination of the molecules' excitation energies. The broad, unresolved peak on the right contains the absorption spectra of the upper polariton and two other energy eigenstates that mainly consist of molecular degrees of freedom.

The energy of the LP is obtained by diagonalizing the Hamiltonian of the molecule-cavity system, which in this case is a 4×4 matrix

$$\begin{pmatrix} \omega_{\rm c} & \Omega_{\rm R}^{(1)}/2 & \Omega_{\rm R}^{(2)}/2 & \Omega_{\rm R}^{(3)}/2 \\ \Omega_{\rm R}^{(1)}/2 & \omega_1 & V_{12} & V_{13} \\ \Omega_{\rm R}^{(2)}/2 & V_{21} & \omega_2 & V_{23} \\ \Omega_{\rm R}^{(3)}/2 & V_{31} & V_{32} & \omega_3 \end{pmatrix}. \tag{7}$$

The deviation of the position of the LP peak in the absorption spectrum from the LP energy was determined to be $|\nu_{\rm LP} - \omega_{\rm LP}| \simeq 19\,{\rm cm}^{-1}$. By repeating the measurement of the lower polariton energy with variable molecular density and/or variable cavity frequency, for example, by adjusting the distance between two mirrors and using the genetic algorithm for a multivariable fitting [11,63–65], the excitation energies of the molecules can be determined or at least the accuracy of their values obtained by using other approaches can be evaluated.

IV. CAVITY-TRANSMISSION SPECTRUM

Next, we consider an ensemble of N identical molecules with different orientations coupled to a single mode of an optical cavity. In this case, the energy of the LP can be

obtained in the same way as the case of a single molecule, by using an effective Rabi coupling

$$\Omega_{\rm R}^{\rm eff} = \sqrt{\sum_{m=1}^{N} \left|\Omega_{\rm R}^{(m)}\right|^2}, \tag{8}$$

where $\Omega_{\rm R}^{(m)}$ is the Rabi coupling associated with the mth molecule. If the orientations of the molecules are random, by taking an average over all possible directions $\langle \cos^2\theta \rangle_\theta = 1/2$, we obtain $\Omega_{\rm R}^{\rm eff} = |\Omega_{\rm R}|\sqrt{N/2}$, where $\Omega_{\rm R}$ is the Rabi coupling of a single molecule.

Similarly, if an ensemble of N identical molecular complexes with different orientations is coupled to a single mode of an optical cavity, the energy of the LP can be obtained in the same way as the case of a single molecular complex, by using effective Rabi frequencies for excitation energy eigenstates (excitons) of the molecular complex

$$\Omega_{\rm R}^{i,\rm eff} = \sqrt{\sum_{m=1}^{N} \left|\Omega_{\rm R}^{i,(m)}\right|^2}. \tag{9}$$

Here the superscript i labels the excitons of each molecular complex, and $\Omega_{\rm R}^{i,(m)}$ represents the Rabi coupling associated with the ith exciton in the mth molecular complex. Due to electronic coupling between molecules, the excitons are in general superpositions of electronic excitations of different molecules in the complex. If the orientations of molecular complexes are random, the effective Rabi couplings reduce to $\Omega_{\rm R}^{i,\rm eff} = |\Omega_{\rm R}^{i}|\sqrt{N/2}$, where $\Omega_{\rm R}^{i}$ is the Rabi coupling associated with the ith exciton in a single molecular complex. It should be noted that for the purpose of precise determination of excitation energies in a single molecule or molecular complex, a sufficiently dilute ensemble of identical molecules or molecular complexes should be used so that the interaction between molecules or between molecular complexes is negligibly small. However, it is clear from the LP linewidth for $N = 1$ shown in Fig. 2 that even in the limiting case of a single molecule or molecular complex strongly coupled to an optical cavity mode, the resulting LP has a smaller linewidth than that of the bare molecules. This implies that a precise determination of excitation energies is feasible even if the molecular system contains only a single molecule or molecular complex.

In the preceding sections, we have demonstrated that the sharp and isolated peak of LP appears in the molecular-absorption spectrum, which can be used for precise determination of molecular excitation energies. However, if there are pairs of identical molecules with opposite orientations such that their Rabi couplings have the same magnitude but the opposite signs, the LP would become a dark state with respect to molecular absorption. This situation is encountered especially in a system of identical molecules or molecular complexes with random orientations. In this case, given that the polariton always involves the degrees of freedom of the cavity, its energy can be obtained from cavity-transmission spectroscopy measurements.

For a numerical demonstration of the cavity-transmission spectrum, we consider a system of $N = 4$ identical molecules that form two pairs of molecules with opposite orientations.

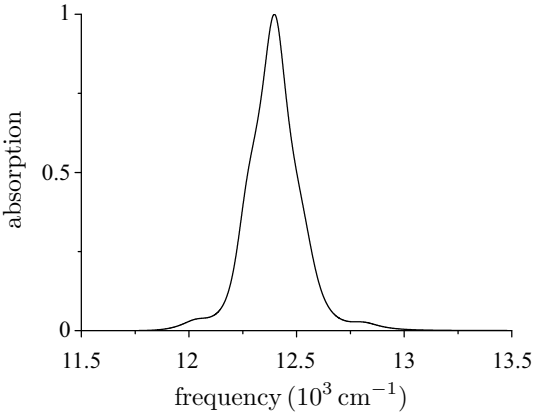

FIG. 9. Molecular-absorption spectrum of a system of $N = 4$ identical molecules that form two pairs of molecules (1,2) and (3,4) oriented in the opposite directions. The Rabi couplings are $\sqrt{N}\Omega_{\rm R}^{(1)} = 0.1$ eV, $\Omega_{\rm R}^{(2)} = -\Omega_{\rm R}^{(1)}$, $\Omega_{\rm R}^{(3)} = \Omega_{\rm R}^{(1)}\sqrt{3}/2$, and $\Omega_{\rm R}^{(4)} = -\Omega_{\rm R}^{(3)}$. The molecular excitation energy is $\omega_0 = 12\,400\ {\rm cm}^{-1}$ and the cavity frequency is $\omega_{\rm c} = 12\,450\ {\rm cm}^{-1}$. The parameters of the environment are the same as those given in Fig. 8.

As a result, the Rabi couplings satisfy $\Omega_{\rm R}^{(2)} = -\Omega_{\rm R}^{(1)}$ and $\Omega_{\rm R}^{(4)} = -\Omega_{\rm R}^{(3)}$. In this case, we take $\sqrt{N}\Omega_{\rm R}^{(1)} = 0.1$ eV and $\Omega_{\rm R}^{(3)} = \Omega_{\rm R}^{(1)}\sqrt{3}/2$. The other parameters of the system and the environment are the same as those of the aforementioned system that was investigated. The molecular-absorption spectrum is shown in Fig. 9. It is clearly seen that the main peak appears around the bare molecular excitation energy $\omega_0 = 12400\,{\rm cm}^{-1}$. This peak is broad with a linewidth of approximately $227\,{\rm cm}^{-1}$. It contains the absorption spectrum of three energy eigenstates other than the polaritons. On both sides of the main peak there exist two very small peaks which should be attributed to the lower and upper polaritons. In the absence of thermal fluctuation, the two polaritons are completely dark with respect to molecular absorption. However, thermal fluctuation induced by the environment can affect the structure of the polaritons, by which the polaritons become not fully dark states.

Next, we consider the cavity transmission spectroscopy of the above molecular system with an optical cavity consisting of two mirrors with loss rates $\kappa_1 = \kappa_2 = \kappa$. The input and output field operators are related to each other by the boundary condition at each mirror as given by

$$\hat{a}_{\rm in}^{(i)}(t) + \hat{a}_{\rm out}^{(i)}(t) = \sqrt{\kappa_i}\hat{a}(t), \tag{10}$$

where $i = 1, 2$ and the operators are those in the Heisenberg picture. For the cavity-transmission measurement, we consider a coherent input field at the left mirror ($i = 1$) as described by the operator

$$\hat{V}_{\rm p} = \hbar A_{\rm p}(e^{-i\omega_{\rm p}t}\hat{a}^\dagger + e^{i\omega_{\rm p}t}\hat{a}), \tag{11}$$

where $A_{\rm p}$ and $\omega_{\rm p}$ represent the amplitude and frequency of the input field, respectively. The total power $I = \int d\omega S_{\rm ss}(\omega)$ of the output field at the right mirror ($i = 2$) is measured, where

$$S_{\rm ss}(\omega) = \lim_{t\to\infty} \int_{-\infty}^{\infty} d\tau\, e^{-i\omega\tau} \left\langle \hat{a}_{\rm out}^{(2)}(t+\tau)^\dagger \hat{a}_{\rm out}^{(2)}(t) \right\rangle \tag{12}$$

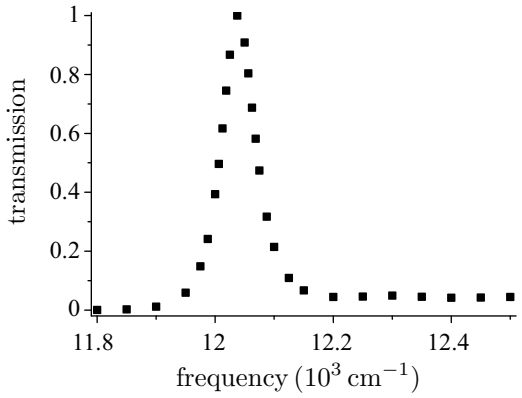

FIG. 10. Cavity-transmission spectrum of the same molecular system as in Fig. 9.

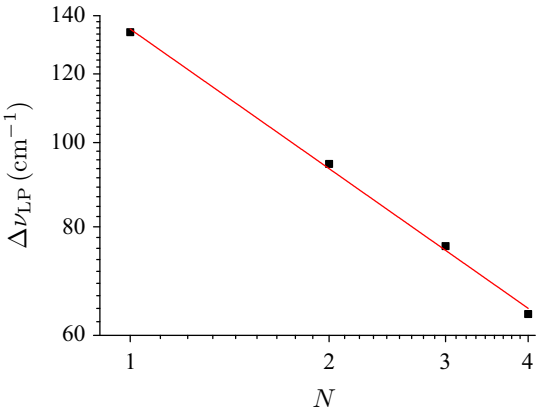

FIG. 11. Dependence of the linewidth $\Delta\nu_{\rm LP}$ of the LP peak in the cavity-transmission spectrum on the number N of molecules coupled to the cavity mode. Here both axes are shown in logarithmic scales. The red line is the linear fitting of the numerical data.

is the power spectrum at the steady state. Since the input field at the right mirror is in the vacuum state, the power spectrum of the output field is proportional to that of the cavity field,

$$\left\langle \hat{a}^{(2)}_{\rm out}(t+\tau)^\dagger \hat{a}^{(2)}_{\rm out}(t)\right\rangle = \kappa_2 \langle \hat{a}(t+\tau)^\dagger \hat{a}(t)\rangle. \tag{13}$$

As a result, the total power of the output field is proportional to the number of photons in the cavity at the steady state, $\lim_{t\to\infty}\langle \hat{a}(t)^\dagger \hat{a}(t)\rangle$. The time-dependent cavity field is obtained by solving the quantum master equation [66].

The cavity-transmission spectrum is shown in Fig. 10. It is clear that there is a relatively sharp peak of LP with a linewidth of $\Delta\nu_{\rm LP} \simeq 67\,{\rm cm}^{-1}$, which is comparable in magnitude with that in the molecular-absorption spectrum of a system of $N = 4$ molecules with the same orientation (see Fig. 2). There is also a very small and flat transmission spectrum around $12400\,{\rm cm}^{-1}$ due to the three energy eigenstates of the system that mainly consist of molecular degrees of freedom. In the absence of thermal fluctuation induced by the environment, these eigenstates do not appear in the cavity-transmission spectrum. Their signals in the cavity-transmission spectrum should therefore be attributed to the effect of thermal fluctuations, which affect the structures of these eigenstates by inducing small mixing of the degrees of freedom of light and matter.

By investigating the LP linewidth as a function of N, it is determined that the power scaling law $\Delta\nu_{\rm LP} \propto N^{-\alpha}$ also holds for the cavity-transmission measurement as shown in Fig. 11 for $\sqrt{N}\Omega_{\rm R} = 0.1\,{\rm eV}$, with the obtained LP linewidth $\Delta\nu_{\rm LP}$ and the exponent $\alpha = 0.53 \pm 0.02$ close to those obtained from molecular-absorption measurement. This implies that the power scaling law is a universal feature of the molecular polariton system which does not depend on the experimental method used to measure it [67].

V. CONCLUSIONS

We have demonstrated that a precise determination of the excitation energies of condensed-phase molecular systems is possible by strongly coupling the molecules to an optical cavity and measuring the energy of the LP, which is a mixture of light and matter degrees of freedom. The LP linewidth is determined to exhibit a power scaling with respect to the number of molecules coupled to the cavity mode. The power exponent strongly depends on the environment's dynamic timescale. Therefore, the environmental dynamics information can be extracted from the LP spectrum measured for a variable number of molecules. The exciton-polariton-based approach proposed here is the first step in the development of new methods for precise measurement and/or control of various physical properties of condensed-phase molecular systems [68,69], which is significant from the perspective of both fundamental science and technological application.

ACKNOWLEDGMENTS

This work was supported by JSPS KAKENHI Grants No. 19K14638 (N.T.P.), No. 17H02946, and No. 18H01937, and JSPS KAKENHI Grant No. 17H06437 in Innovative Areas "Innovations for Light-Energy Conversion (I^4LEC)" (A.I.).

[1] V. May and O. Kühn, *Charge and Energy Transfer Dynamics in Molecular Systems*, 3rd ed. (Wiley-VCH, Weinheim, Germany, 2011).

[2] A. Nitzan, *Chemical Dynamics in Condensed Phases: Relaxation, Transfer and Reactions in Condensed Molecular Systems* (Oxford University, Oxford, 2006).

[3] J. Eccles and B. Honig, Charged amino acids as spectroscopic determinants for chlorophyll in vivo, Proc. Natl. Acad. Sci. USA **80**, 4959 (1983).

[4] A. Damjanovic, H. M. Vaswani, P. Fromme, and G. R. Fleming, Chlorophyll excitations in photosystem I of Synechococcus elongatus, J. Phys. Chem. B **106**, 10251 (2002).

[5] D. Spangler, G. M. Maggiora, L. L. Shipman, and R. E. Christoffersen, Stereoelectronic properties of photosynthetic and related systems. 2. Ab initio quantum mechanical ground state characterization of magnesium porphine, magnesium chlorin, and ethyl chlorophyllide-a, J. Am. Chem. Soc. **99**, 7478 (1977).

[6] J. N. Sturgis and B. Robert, The role of chromophore coupling in tuning the spectral properties of peripheral light-harvesting protein of purple bacteria, Photosynth. Res. **50**, 5 (1996).

[7] J. N. Sturgis and B. Robert, Pigment binding-site and electronic properties in light-harvesting proteins of purple bacteria, J. Phys. Chem. B **101**, 7227 (1997).

[8] H. Witt, E. Schlodder, C. Teutloff, J. Niklas, E. Bordignon, D. Carbonera, S. Kohler, A. Labahn, and W. Lubitz, Hydrogen bonding to P700: site-directed mutagenesis of threonine A739 of Photosystem I in Chlamydomonas reinhardtii, Biochemistry **41**, 8557 (2002).

[9] A. Warshel and W. W. Parson, Spectroscopic properties of photosynthetic reaction centers. I. Theory, J. Am. Chem. Soc. **109**, 6143 (1987).

[10] E. Gudowska-Nowak, M. D. Newton, and J. Fajer, Conformational and environmental effects on bacteriochlorophyll optical spectra: correlations of calculated spectra with structural results, J. Phys. Chem. **94**, 5795 (1990).

[11] J. Adolphs and T. Renger, How proteins trigger excitation energy transfer in the FMO complex of green sulfur bacteria, Biophys. J. **91**, 2778 (2006).

[12] A. Ishizaki and G. R. Fleming, Theoretical examination of quantum coherence in a photosynthetic system at physiological temperature, Proc. Natl. Acad. Sci. USA **106**, 17255 (2009).

[13] S. I. E. Vulto, M. A. de Baat, M. A. Louwe, H. P. Permentier, T. Neef, M. Miller, H. van Amerongen, and H. P. Aartsma, Exciton simulations of optical spectra of the FMO complex from the green sulfur bacterium Chlorobium tepidum at 6 K, J. Phys. Chem. B **102**, 9577 (1998).

[14] M. Wendling, M. A. Przyjalgowski, D. Gulen, S. I. E. Vulto, T. J. Aartsma, R. van Grondelle, and H. van Amerongen, The quantitative relationship between structure and polarized spectroscopy in the FMO complex of Prosthecochloris aestuarii: Refining experiments and simulations, Photosynth. Res. **71**, 99 (2002).

[15] T. W. Ebbesen, Hybrid light-matter states in a molecular and material science perspective, Acc. Chem. Res. **49**, 2403 (2016).

[16] D. G. Lidzey, D. D. C. Bradley, M. S. Skolnick, T. Virgili, S. Walker, and D. M. Whittaker, Strong exciton-photon coupling in an organic semiconductor microcavity, Nature **395**, 53 (1998).

[17] J. R. Tischler, M. S. Bradley, V. Bulovic, J. H. Song, and A. Nurmikko, Strong Coupling in a Microcavity LED, Phys. Rev. Lett. **95**, 036401 (2005).

[18] R. J. Holmes and S. R. Forrest, Strong exciton-photon coupling in organic materials, Org. Electron. **8**, 77 (2007).

[19] S. Kena-Cohen, M. Davanco, and S. R. Forrest, Strong Exciton-Photon Coupling in an Organic Single Crystal Microcavity, Phys. Rev. Lett. **101**, 116401 (2008).

[20] J. Bellessa, C. Symonds, J. Laverdant, J.-M. Benoit, J. C. Plenet, and S. Vignoli, Strong coupling between plasmons and organic semiconductors, Electronics **3**, 303 (2014).

[21] M. Mazzeo *et al.*, Ultrastrong light-matter coupling in electrically doped microcavity organic light emitting diodes, Appl. Phys. Lett. **104**, 233303 (2014).

[22] J. P. Long and B. S. Simpkins, Coherent coupling between a molecular vibration and Fabry-Perot optical cavity to give hybridized states in the strong coupling limit, ACS Photonics **2**, 130 (2015).

[23] J. George, A. Shalabney, J. A. Hutchison, C. Genet, and T. W. Ebbesen, Liquid-phase vibrational strong coupling, J. Phys. Chem. Lett. **6**, 1027 (2015).

[24] A. Shalabney, J. George, J. Hutchison, G. Pupillo, C. Genet, and T. W. Ebbesen, Coherent coupling of molecular resonators with a microcavity mode, Nat. Commun. **6**, 5981 (2015).

[25] R. Chikkaraddy, B. de Nijs, F. Benz, S. J. Barrow, O. A. Scherman, E. Rosta, A. Demetriadou, P. Fox, O. Hess, and J. J. Baumberg, Single-molecule strong coupling at room temperature in plasmonic nanocavities, Nature **535**, 127 (2016).

[26] J. A. Hutchison, T. Schwartz, C. Genet, E. Devaux, and T. W. Ebbesen, Modifying chemical landscapes by coupling to vacuum fields, Angew. Chem., Int. Ed. **51**, 1592 (2012).

[27] B. S. Simpkins, K. P. Fears, W. J. Dressick, B. T. Spann, A. D. Dunkelberger, and J. C. Owrutsky, Spanning strong to weak normal mode coupling between vibrational and Fabry-Perot cavity modes through tuning of vibrational absorption strength, ACS Photonics **2**, 1460 (2015).

[28] F. Herrera and F. C. Spano, Cavity-Controlled Chemistry in Molecular Ensembles, Phys. Rev. Lett. **116**, 238301 (2016).

[29] J. Galego, F. J. Garcia-Vidal, and J. Feist, Suppressing photochemical reactions with quantized light fields, Nat. Commun. **7**, 13841 (2016).

[30] A. Thomas, J. George, A. Shalabney, M. Dryzhakov, S. J. Varma, J. Moran, T. Chervy, X. Zhong, E. Devaux, C. Genet, J. A. Hutchison, and T. W. Ebbesen, Ground-state chemical reactivity under vibrational coupling to the vacuum electromagnetic field, Angew. Chem. Int. Ed. **55**, 11462 (2016).

[31] A. Thomas, L. Lethuillier-Karl, K. Nagarajan, R. M. A. Vergauwe, J. George, T. Chervy, A. Shalabney, E. Devaux, C. Genet, J. Moran, and T. W. Ebbesen, Tilting a ground-state reactivity landscape by vibrational strong coupling, Science **363**, 615 (2019).

[32] H. Hiura, A. Shalabney, and J. George, Cavity catalysis: Accelerating reactions under vibrational strong coupling, doi: 10.26434/chemrxiv.7234721.v3 (2018).

[33] J. Lather, P. Bhatt, A. Thomas, T. W. Ebbesen, and J. George, Cavity catalysis by cooperative vibrational strong coupling of reactant and solvent molecules, Angew. Chem. Int. Ed. **58**, 10635 (2019).

[34] J. A. Hutchison *et al.*, Tuning the work-function via strong coupling, Adv. Mater. **25**, 2481 (2013).

[35] P. Andrew and W. L. Barnes, Forster energy transfer in an optical microcavity, Science **290**, 785 (2000).

[36] J. Feist and F. J. Garcia-Vidal, Extraordinary Exciton Conductance Induced by Strong Coupling, Phys. Rev. Lett. **114**, 196402 (2015).

[37] J. Schachenmayer, C. Genes, E. Tignone, and G. Pupillo, Cavity-Enhanced Transport of Excitons, Phys. Rev. Lett. **114**, 196403 (2015).

[38] E. Orgiu *et al.*, Conductivity in organic semiconductors hybridized with the vacuum field, Nat. Mater. **14**, 1123 (2015).

[39] J. Yuen-Zhou, S. K. Saikin, T. Zhu, M. C. Onbasli, C. A. Ross, V. Bulovic, and M. A. Baldo, Plexciton Dirac points and topological modes, Nat. Commun. **7**, 11783 (2016).

[40] F. Herrera, B. Peropadre, L. A. Pachon, S. K. Saikin, and A. Aspuru-Guzik, Quantum nonlinear optics with polar J-aggregates in microcavities, J. Phys. Chem. Lett. **5**, 3708 (2014).

[41] K. Bennett, M. Kowalewski, and S. Mukamel, Novel photochemistry of molecular polaritons in optical cavities, Faraday Discuss. **194**, 259 (2016).

[42] M. Kowalewski, K. Bennett, and S. Mukamel, Non-adiabatic dynamics of molecules in optical cavities, J. Chem. Phys. **144**, 054309 (2016).

[43] M. Kowalewski, K. Bennett, and S. Mukamel, Cavity femtochemistry; manipulating nonadiabatic dynamics at avoided crossings, J. Phys. Chem. Lett. **7**, 2050 (2016).

[44] S. Kena-Cohen and S. R. Forrest, Room-temperature polariton lasing in an organic single-crystal microcavity, Nat. Photonics **4**, 371 (2010).

[45] J. A. Cwik, S. Reja, P. B. Littlewood, and J. Keeling, Polariton condensation with saturable molecules dressed by vibrational modes, Europhys. Lett. **105**, 47009 (2014).

[46] G. Lerario, A. Fieramosca, F. Barachati, D. Ballarini, K. S. Daskalakis, L. Dominici, M. De Giorgi, S. A. Maier, G. Gigli, and S. Kena-Cohen, Room-temperature superfluidity in a polariton condensate, Nat. Phys. **13**, 837 (2017).

[47] J. D. Plumhof, T. Stoferle, L. Mai, U. Scherf, and R. F. Mahrt, Room-temperature Bose Einstein condensation of cavity exciton polaritons in a polymer, Nat. Mater. **13**, 247 (2014).

[48] F. C. Spano, Optical microcavities enhance the exciton coherence length and eliminate vibronic coupling in J-aggregates, J. Chem. Phys. **142**, 184707 (2015).

[49] N. Wu, J. Feist, and F. J. Garcia-Vidal, When polarons meet polaritons: Exciton-vibration interactions in organic molecules strongly coupled to confined light fields, Phys. Rev. B **94**, 195409 (2016).

[50] M. A. Zeb, P. G. Kirton, and J. Keeling, Exact states and spectra of vibrationally dressed polaritons, ACS Photonics **5**, 249 (2018).

[51] F. Herrera and F. C. Spano, Theory of nanoscale organic cavities: the essential role of vibration-photon dressed states, ACS Photonics **5**, 65 (2018).

[52] J. del Pino, F. A. Y. N. Schroder, A. W. Chin, J. Feist, and F. J. Garcia-Vidal, Tensor network simulation of polaron-polaritons in organic microcavities, Phys. Rev. B **98**, 165416 (2018).

[53] A. Ishizaki, T. R. Calhoun, G. S. Schlau-Cohen, and G. R. Fleming, Quantum coherence and its interplay with protein environments in photosynthetic electronic energy transfer, Phys. Chem. Chem. Phys. **12**, 7319 (2010).

[54] Y. Tanimura, Stochastic Liouville, Langevin, Fokker-Planck, and master equation approaches to quantum dissipative systems, J. Phys. Soc. Jpn. **75**, 082001 (2006).

[55] S. Mukamel, *Principles of Nonlinear Optical Spectroscopy* (Oxford University, Oxford, 1995).

[56] A. V. Kavokin, J. J. Baumberg, G. Malpuech, and F. P. Laussy, *Microcavities* (Oxford University, Oxford, 2007).

[57] P. W. Anderson, A mathematical model for the narrowing of spectral lines by exchange or motion, J. Phys. Soc. Jpn. **9**, 316 (1954).

[58] J. H. Song, Y. He, A. V. Nurmikko, J. Tischler, and V. Bulovic, Exciton-polariton dynamics in a transparent organic semiconductor microcavity, Phys. Rev. B **69**, 235330 (2004).

[59] T. Virgili, D. Coles, A. M. Adawi, C. Clark, P. Michetti, S. K. Rajendran, D. Brida, D. Polli, G. Cerullo, and D. G. Lidzey, Ultrafast polariton relaxation dynamics in an organic semiconductor microcavity, Phys. Rev. B **83**, 245309 (2011).

[60] T. Schwartz, J. A. Hutchison, J. Léonard, C. Genet, S. Haacke, and T. W. Ebbesen, Polariton dynamics under strong light-molecule coupling, Chem. Phys. Chem. **14**, 125 (2013).

[61] S. Wang, T. Chervy, J. George, J. A. Hutchison, C. Genet, and T. W. Ebbesen, Quantum yield of polariton emission from hybrid light-matter states, J. Phys. Chem. Lett. **5**, 1433 (2014).

[62] A. Canaguier-Durand, C. Genet, A. Lambrecht, T. W. Ebbesen, and S. Reynaud, Non-Markovian polariton dynamics in organic strong coupling, Eur. Phys. J. D **69**, 24 (2015).

[63] W. Kinnebrock, *Optimierung mit genetischen und selektiven Algorithmen (Optimization with genetic and selective algorithms)* (Oldenbourg, Germany, 1994).

[64] H. Pohlheim, *Evolutionare Algorithmen (Evolutionary algorithms)* (Springer, Berlin, 1999).

[65] B. Bruggemann, K. Sznee, V. Novoderezhkin, R. van Grondelle, and V. May, Modeling exciton dynamics in the photosynthetic antenna PS1, J. Phys. Chem. B **108**, 13536 (2004).

[66] D. F. Walls and G. J. Milburn, *Quantum Optics*, 2nd ed. (Springer-Verlag, Berlin, 2008).

[67] F. Herrera and F. C. Spano, Absorption and photoluminescence in organic cavity QED, Phys. Rev. A **95**, 053867 (2017).

[68] N. T. Phuc and A. Ishizaki, Control of excitation energy transfer in condensed phase molecular systems by Floquet engineering, J. Phys. Chem. Lett. **9**, 1243 (2018).

[69] N. T. Phuc and A. Ishizaki, Control of quantum dynamics of electron transfer in molecular loop structures: Spontaneous breaking of chiral symmetry under strong decoherence, Phys. Rev. B **99**, 064301 (2019).